

Vector Control of Three Phase Squirrel Cage Induction Motor based on Internet of Things

Muldi Yuhendri

Department of Electrical Engineering, Faculty of Engineering, Universitas Negeri Padang, Indonesia
muldiy@ft.unp.ac.id (corresponding author)

Yulianta Siregar

Department of Electrical Engineering, Faculty of Engineering, Universitas Sumatera Utara, Indonesia
julianta_srg@usu.ac.id

Deded Candra Riawan

Department of Electrical Engineering, Institut Teknologi Sepuluh Nopember, Indonesia
dedet.riawan@its.ac.id

Nur Nabila Mohamed

College of Engineering, University Technology MARA, Shah Alam, Malaysia
nurnabilamohamed@uitm.edu.my

Taali

Department of Electrical Engineering, Faculty of Engineering, Universitas Negeri Padang, Indonesia
taaliftunp@gmail.com

Fatimah Hanifah

Department of Electrical Engineering, Faculty of Engineering, Universitas Negeri Padang, Indonesia
fatimahhanifah175@gmail.com

Received: 30 November 2024 | Revised: 21 February 2025 | Accepted: 24 February 2025

Licensed under a CC-BY 4.0 license | Copyright (c) by the authors | DOI: <https://doi.org/10.48084/etasr.9790>

ABSTRACT

Electric motors, which are widely used in industry, need to be controlled and monitored to ensure that they operate as intended. With the development of Internet of Things (IoT) technology, electric motors can be remotely controlled and accurately monitored in real time. This paper proposes an IoT-based supervised control of a three-phase Squirrel Cage Induction Motor (SCIM) using a Variable Speed Drive (VSD) module and a Programmable Logic Controller (PLC) as a control device with several display screens, namely Human Machine Interface (HMI), PC server, and PC client. This allows the electric motor to be remotely controlled and monitored via the internet by a motor control system implemented using the vector control method available in the VSD module. The proposed method has been verified through laboratory experiments, and the experimental results demonstrate that the IoT-based supervised control system of the induction motor works as designed. The motor rotation speed and direction can be successfully controlled and monitored according to the reference using the HMI, PC server, and PC client.

Keywords-vector control; squirrel cage induction motor; Internet of Things; PLC; HMI

I. INTRODUCTION

Electric motors can be considered the heart of industrial production processes, since a wide variety of industrial equipment uses electric motors as a power source for both linear motion and rotary motion. Three-phase SCIMs are one of the most widely used motors in industry, especially for high

power and high rotational speed applications, such as pumps, conveyors, compressors [1-2]. It is well known that SCIMs have several advantages over other types of electric motors, such as simple brushless construction for greater durability, high efficiency especially at full load, and lower purchase and maintenance costs than other types of electric motors [3-5].

Electric motors used in industry must operate accurately and reliably to maintain production quality. To achieve this goal, the motor must be continuously controlled and monitored in real time via appropriate control devices and control methods. Motor control includes the regulation of rotation speed, direction of rotation, and braking and starting current for large power motors [6]. With the development of technology, the development of motor control devices has also progressed. In the early era, manual switches were used for motor control, which was followed by the utilization of electromagnetic switches. Today, motor control has widely used power semiconductors packaged in the form of power converters. Power converters provide regulation of voltage, current, and frequency, making it possible to control motor speed, direction of rotation, and braking. The type of power converter used for SCIM control is the inverter. In this paper, a three-phase inverter module is proposed to control a three-phase SCIM, known as a VSD module or a Variable Frequency Drive (FVD) module [7, 8]. The type of VSD used is Sinamic G120, which is compatible with three-phase SCIMs.

The reliability of the SCIM control system is also determined by the control method of the motor. In general, SCIM control methods are divided into scalar control and vector control [9-11]. Scalar control, also known as volt-hertz control, is a method of controlling the speed of an induction motor by regulating the scalar quantities of voltage and frequency via a power converter [12]. The advantages of this method are that it is simple, easy, and inexpensive to implement. However, it has the disadvantage of being inaccurate and less stable under dynamic loads, making it suitable for implementation only in applications that do not require high control precision [13]. To overcome the weaknesses of scalar control, many vector control schemes have been developed in SCIM. Typically, vectors are divided in Direct Torque Control (DTC) and Field Oriented Control (FOC) [14-16]. DTC has a simpler structure, but is less reliable than FOC in handling load dynamics. On the other hand, FOC is more reliable in handling the dynamics of external disturbances while being more sophisticated. In contrast to DTC, FOC is a vector control technique that uses indirect torque and flux regulation - where torque and flux are controlled by the stator current in the dq-axes - to control the speed of an electric motor [17-20]. In this paper, the SCIM control method based on FOC implemented in the Sinamic G120 VSD module is used.

The development of the internet allows the implementation of supervised control systems in SCIMs, increasing the reliability of SCIM control systems. The utilization of the IoT technology allows SCIMs to be remotely controlled and monitored, making them more flexible to use [21]. Several devices have been employed for IoT-based SCIM control, such as PLC [22-23], VLT302 drives [24], Arduino microcontrollers with Nodem MCU, and ESP 32 [25-30]. Microcontrollers are widely used because they are inexpensive, but their capacity is limited, unlike PLCs, which are expensive but have larger capacity. In this study, an IoT-based vector control system for SCIM was developed using the Siemens S7 1200 PLC. The system is equipped with an HMI display, a PC server, and a PC client for monitoring and controlling the SCIM. The PC server

is also equipped with a data logger that allows operators to view historical data. This design is expected to increase the reliability and flexibility of IoT-based SCIM control.

II. METHODOLOGY

Vector control is a speed control method that decouples the torque and flux control on the SCIM so that they can be controlled separately, similar to the control on a DC motor. DTC is a speed control system through direct electromagnetic torque and flux linkage settings, while torque and flux linkage control in the FOC method is performed indirectly through the dq-axis stator current [31-32].

A. Squirrel Cage Induction Motor

Three-phase SCIM can be represented in three-phase axes or in dq-axes. In vector control, SCIM is modeled in dq-axes. The dq-axes SCIM model is illustrated by the equivalent circuit in Figure 1.

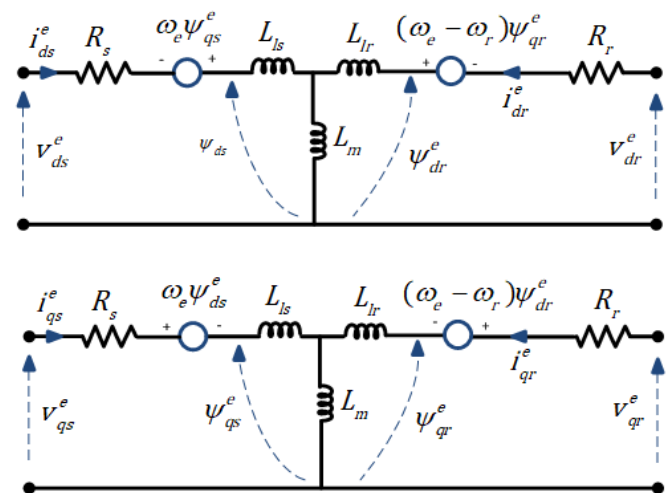


Fig. 1. Equivalent circuit of SCIM in dq-axes.

The speed control of the SCIM model with the FOC method is performed by regulating the flux and torque through the dq-axis current, where the q-axis current represents the torque component and the d-axis current represents the flux component [33]. The SCIM will rotate according to the setpoint value when the electromagnetic torque T_e generated by the SCIM is equal to the torque required by the load T_L at that speed. This can be derived from the following SCIM mechanical dynamics equation:

$$T_e = M \frac{d\omega_m}{dt} + D\omega_m + T_L \quad (1)$$

where D is the friction coefficient and M is the moment of inertia. The electromagnetic torque T_e that must be produced by the SCIM to serve the load is formulated as:

$$T_e = \frac{3}{2} nL_m (i_{qs}^e i_{dr}^e - i_{ds}^e i_{qr}^e) \quad (2)$$

where n is the pole pair number of the SCIM. The electrical power required by the SCIM to move the load P_{in} and the mechanical power produced by SCIM P_{out} are formulated as:

$$P_m = \frac{3}{2}(v_{ds}i_{ds} + v_{qs}i_{qs}) \quad (3)$$

$$P_{out} = T_e \omega_m$$

B. Field Oriented Control of Squirrel Cage Induction Motor

The proposed SCIM control system uses the Sinamic G120 VSD module, which is compatible with the FOC vector control. Figure 2 shows the FOC scheme for the SCIM control system.

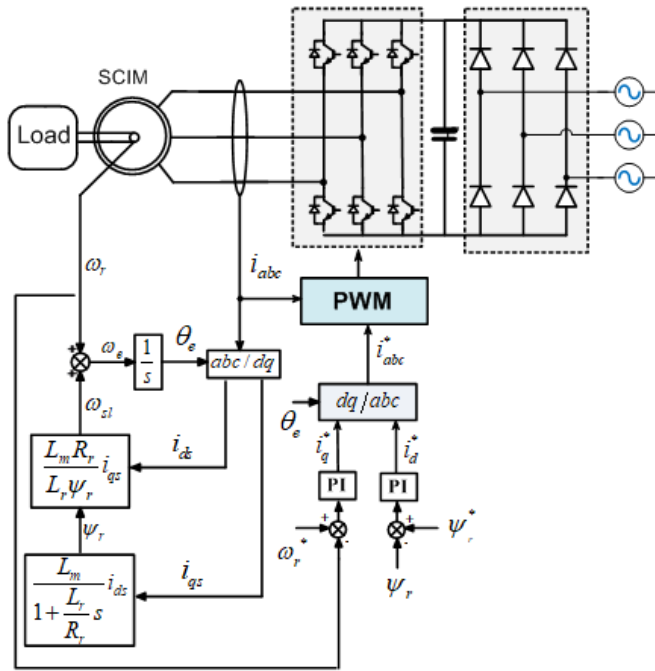


Fig. 2. FOC scheme of the SCIM control system.

The SCIM speed is controlled by regulating the flux and torque through the dq-axis current control. The q-axis current represents the torque parameter, whereas the d-axis current represents the flux parameter, each expressed as:

$$i_{qs}^* = \frac{2}{3} \frac{2}{p} \frac{L_r}{L_m} \frac{T_e^*}{|\psi_r|} \quad (4)$$

$$i_{ds}^* = \frac{\psi_r^*}{L_m}$$

The reference stator currents in the dq-axes i_{qs}^* and i_{ds}^* are obtained from the PI controller, as depicted in Figure 2. The SCIM speed ω_r will match the reference speed ω_r^* when the SCIM currents i_{qs} and i_{ds} are equal to i_{qs}^* and i_{ds}^* . This can be achieved by setting the Pulse Width Modulation (PWM) based on the Hysteresis Current Control (HCC) concept. HCC PWM works on the basis of the current error in the abc axis.

Therefore, the dq-axis reference current from the PI controller must be transformed to the abc axis using the equation:

$$\begin{bmatrix} i_a^* \\ i_b^* \\ i_c^* \end{bmatrix} = \begin{bmatrix} \cos(\theta) & -\sin(\theta) \\ \cos(\theta - 2\pi/3) & \sin(\theta - 2\pi/3) \\ \cos(\theta + 2\pi/3) & \sin(\theta + 2\pi/3) \end{bmatrix} \begin{bmatrix} i_{ds}^* \\ i_{qs}^* \end{bmatrix} \quad (5)$$

where θ is the rotor angle of the SCIM obtained from the equation:

$$\theta = \int (\omega_m + \omega_{s1}) dt \quad (6)$$

$$\omega_{s1} = \frac{L_m R_r}{|\psi_r| L_r} i_{qs} \quad (7)$$

$$|\psi_r| = \frac{L_m i_{ds}}{1 + \frac{L_r}{R_r} s} \quad (8)$$

where ω_{s1} and ψ_r are the slip speed of SCIM and rotor flux, respectively. The FOC design on the Sinamic G120 VSD module is implemented through the TIA portal application software.

C. Internet of Things

Vector control with the FOC method is implemented based on IoT using PLC S7 1200 as the control center and several displays consisting of HMI TP 700 comfort, PC server, and PC client as tools to perform control actions and monitor control parameters. The PC server is equipped with the TIA portal software and Wincc unified PC for IoT applications. The PC server is also equipped with a data logger to store monitored data. The control actions that can be performed include setting the speed and direction of rotation, whereas monitored parameters involve rotation speed, current, voltage, and frequency. These parameters can be obtained through the address on the VSD. Two types of data communication are used, namely the ethernet cable connecting the PLC, the HMI, the PC server, and the VSD, and the internet connecting the PC server and the PC client. Figure 3 illustrates the proposed IoT scheme.

III. RESULTS AND DISCUSSION

The IoT-based vector control design is implemented on a three-phase SCIM with a power rating of 0.75 kW. The SCIM is connected to a Synchronous Generator (SG), where the generator serves a variable resistor load. Figure 4 shows the hardware setup for the experiment.

The first experiment was conducted with a reference speed of 500 rpm in a clockwise (CW) direction. The reference speed was set via the HMI screen. Figure 5 portrays the screen display of the PC server, PC client, and HMI in this first experiment. Figure 5 demonstrates that all displays show the motor speed value of 500 rpm in a CW direction. When the SCIM is operating at 500 rpm, the RMS stator current is 0.3 A, the stator voltage is 120 V, and the frequency is 18 Hz. These

results indicate that the designed IoT system for the VSD of SCIM based on the FOC method has successfully controlled SCIM according to the reference speed and also successfully displayed all the monitored data, namely rotor rotation speed, rotation direction, stator voltage, stator current, and frequency. The data from the tachometer measuring device and the rotor rotation speed data from the speed sensor, which are displayed on all screens, have the same value. The current, voltage, and frequency parameters also yield the same results, with the numbers displayed on all screens matching the values read on the tachometer. These results indicate that the IoT system designed to display the SCIM parameters worked well. The SCIM can also be controlled from all screens, whether from the HMI, the PC server, or the PC client. This shows that the IoT system for Sinamic G120 using the Wincc application has worked well. Even if the control system is operated from different types of screens at different distances, it can react quickly. Depending on the setpoints entered on the screen, the system can execute control operations rapidly.

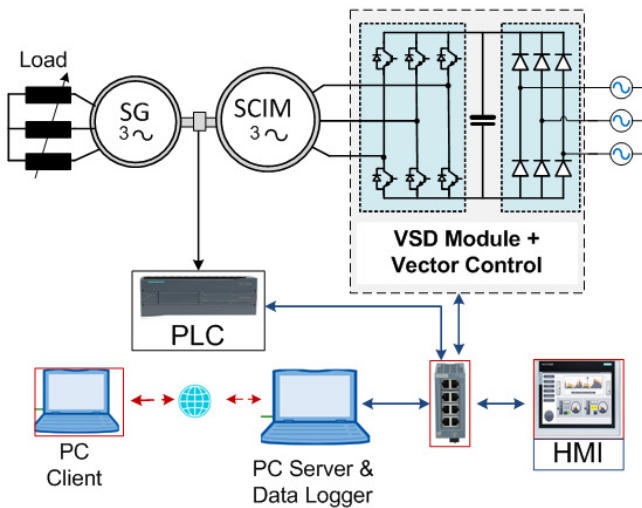


Fig. 3. Proposed IoT scheme.

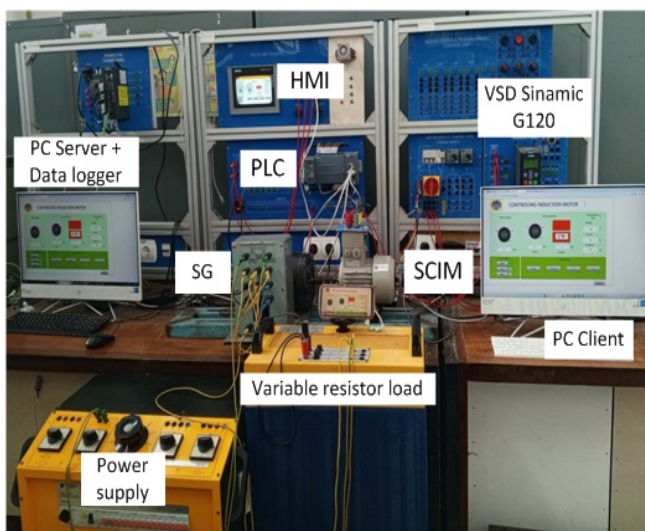
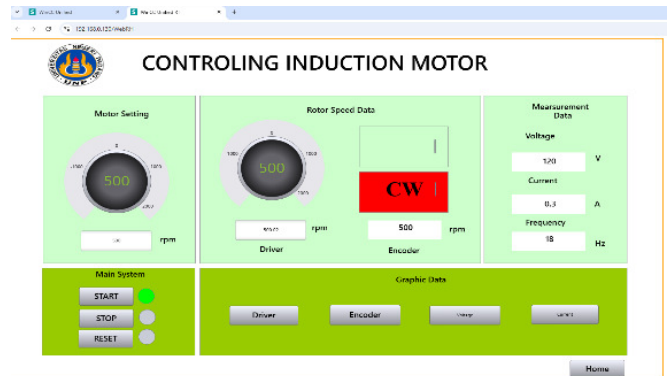
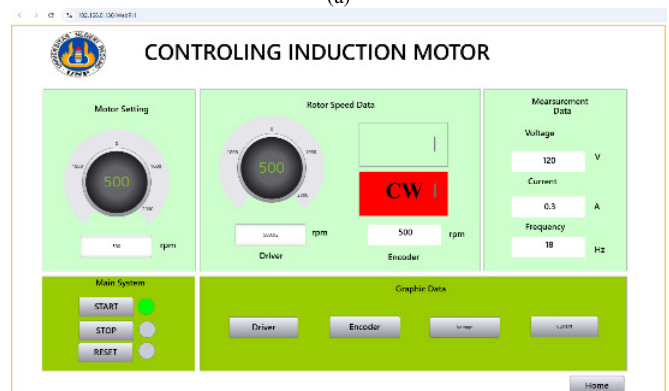


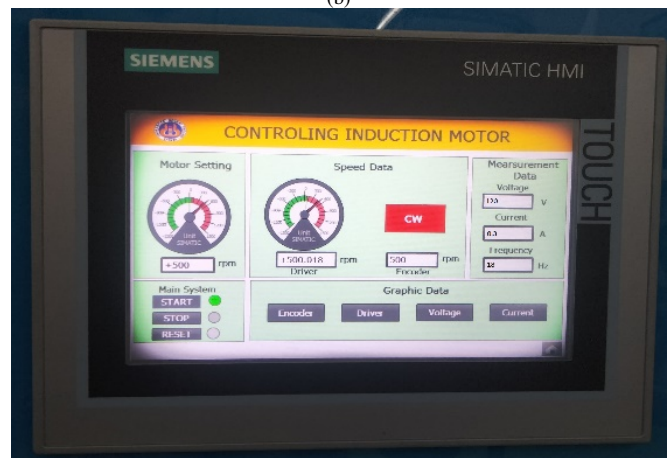
Fig. 4. Experimental setup.



(a)



(b)



(c)

Fig. 5. Results of the first experiment: (a) server, (b) client, and (c) HMI.

The design of the SCIM rotation speed control system using the FOC method based on the PI controller applied to the Sinamic G120 VSD has successfully regulated the motor speed according to its reference value, as indicated by the speed graph presented on the HMI screen in Figure 6. Figure 6 demonstrates that after 4 s of operation the SCIM rotor rotation speed is set to 500 rpm and that the system must run for 7 s before the rotor rotation speed reaches the setpoint. This shows that the SCIM speed can reach the setpoint within 3 s. In addition to quickly reaching the setpoint, the proposed design of the FOC method has also been able to reduce overshoot in transient conditions and has also successfully reduced ripples in

steady-state conditions. As a result, the SCIM speed can be stable according to the reference value, as illustrated in Figure 6.

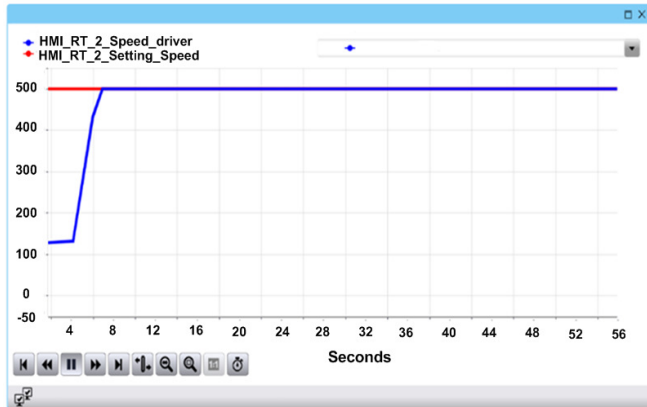


Fig. 6. Speed graph on the HMI screen.

Further experiments were conducted by treating the SCIM at varying reference speeds while keeping the SCIM load in the form of a SG constant. The SCIM rotor speed was varied from 500 rpm to 1000 rpm. Figure 7 presents the result data from the second experiment stored in the data logger on the PC server. Figure 7(a) shows the motor speed data, where the actual motor speed obtained from the speed sensor demonstrates the same value as the reference speed value entered on the HMI screen. In this experiment, the soft starting method is applied by setting the SCIM reference speed with a rise time of 2 s to reduce the starting current. This can be seen in the current graph depicted in Figure 7(b). When the speed changes from 500 rpm to 1000 rpm, there is a transient condition in the current with a slight spike. This would be different if the reference speed was not added with a rise time to reach its setpoint. Figure 7(c) exhibits the graph of the stator RMS voltage in the second experiment. When the speed is 500 rpm, the stator voltage is 120 V and increases to around 210 V when the SCIM speed changes to 1000 rpm. The same is true for the frequency value. The SCIM frequency is around 18 Hz when the motor operates at 500 rpm and then increases to 38 Hz when the SCIM operates at 1000 rpm. Based on these data, it can be seen that the SCIM speed control with the FOC method is done by adjusting the torque and flux through the stator current control. This stator current control is done indirectly by changing the voltage and frequency values by changing the modulation pulse of the PWM generated by the controller. The results of this second experiment indicate that the FOC controller design set via the TIA portal has successfully controlled the SCIM speed under various conditions. These results also show that the data logger design set up on the PC server also worked well and successfully stored the measurement data with a sampling time of 0.1 s.

The third experiment was conducted with varying loads and constant speed. In this experiment, a variable resistive load was applied to the SG connected to the SCIM. The SCIM speed was kept constant at 1000 rpm, whereas the load was varied to approach 2 A and 1 A. Figure 8 presents the results of the

experiment stored on the PC server. Figure 8(a) shows that the SCIM speed remains constant even though the load is changed. Figure 8(b) displays the current graph generated due to changes in load, and Figure 8(c) shows the voltage graph generated due to changes in load. The results of this experiment show that the SCIM speed remains controlled even though the load changes. This demonstrates that the FOC control design is reliable in controlling the SCIM speed under various conditions. All the test results indicate that the vector control design with the IoT-based FOC method has worked well according to its objectives. The IoT system has successfully controlled and monitored the SCIM from various screens. The FOC design has also successfully controlled the motor speed under various conditions.

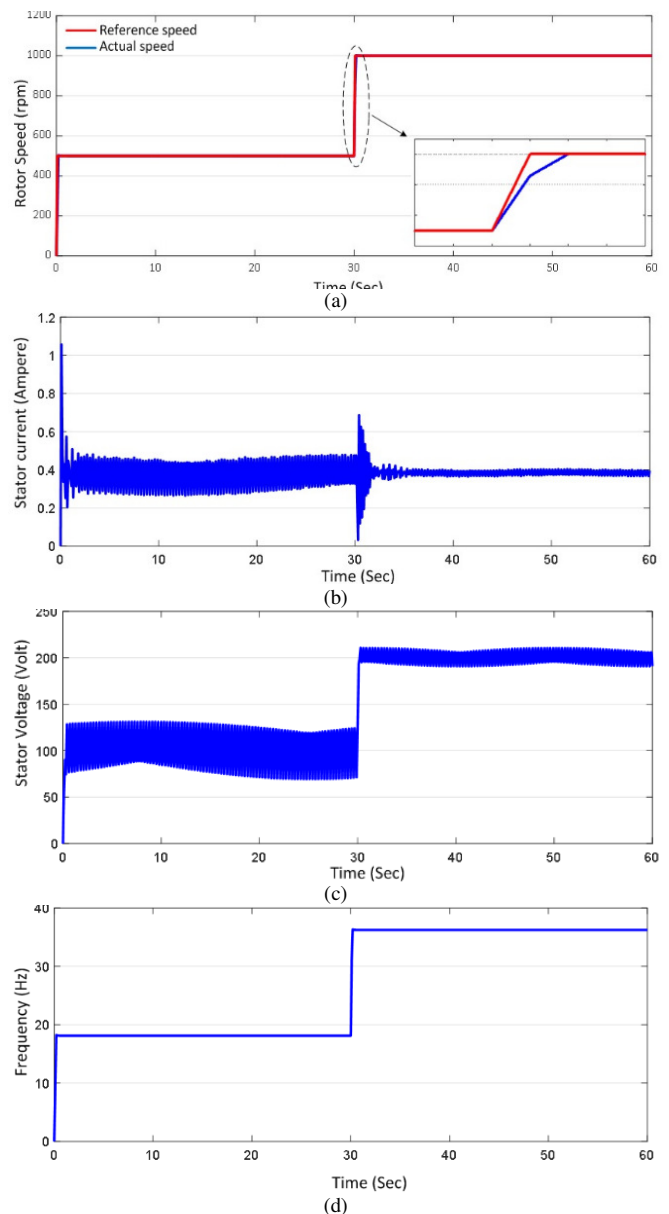


Fig. 7. Results of the second experiment: (a) rotor speed, (b) current, (c) voltage, and (d) frequency.

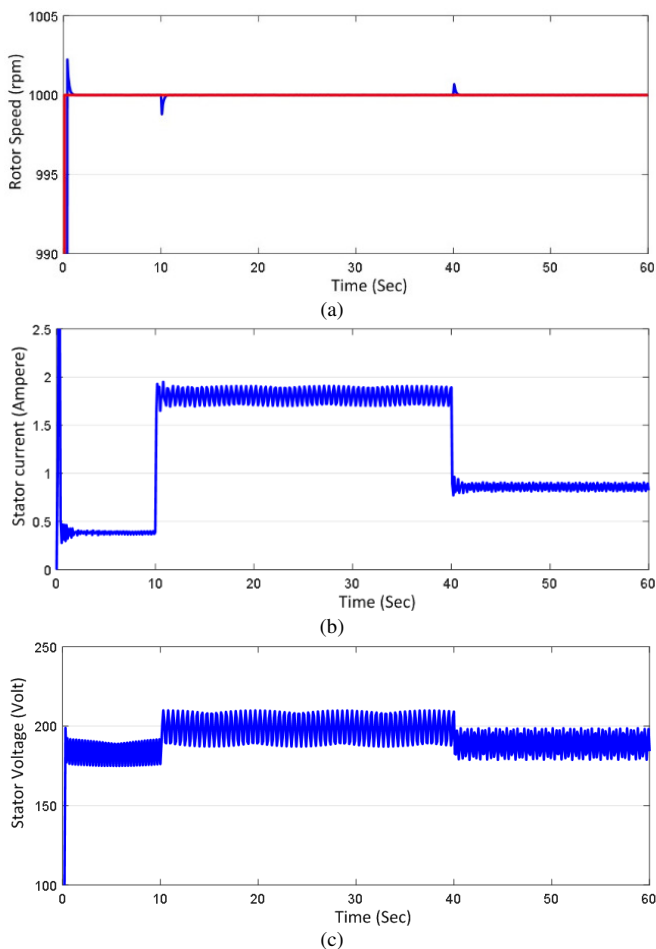


Fig. 8. Results of the third experiment: (a) rotor speed, (b) current, and (c) voltage.

IV. CONCLUSION

This paper proposes the implementation of Internet of Things (IoT)-based vector control using Sinamic G120 Variable Speed Drive (VSD). The vector control is designed deploying the Field Oriented Control (FOC) method based on the PI controller. The IoT system is implemented using the Wincc application with hardware PLC S7 1200, Human Machine Interface (HMI), PC server, and client. The test results show that the proposed vector control with the FOC method has worked well in controlling the motor speed. The FOC method based on the PI controller applied to the Sinamic G120 VSD produced a fast rotor speed response, reaching the setpoint with minimal overshoot in transient conditions and producing a stable response in steady-state conditions. The motor speed was successfully controlled both at varying speeds and under varying load conditions. The created IoT system has also worked well, where the motor can be controlled and monitored from different devices, namely HMI, PC server, and PC client. The IoT system has successfully displayed voltage, current, and frequency data, and has also been successfully stored in the PC server. This proposed IoT system allows the motor to be remotely controlled and monitored via the internet.

ACKNOWLEDGMENT

The authors would like to thank Lembaga Penelitian dan Pengabdian Masyarakat Universitas Negeri Padang for funding this work with a contract number: 1166/UN35.15/LT/2024.

REFERENCES

- [1] B. Wang, J. Zhang, Y. Yu, X. Zhang, and D. Xu, "Unified Complex Vector Field-Weakening Control for Induction Motor High-Speed Drives," *IEEE Transactions on Power Electronics*, vol. 36, no. 6, pp. 7000–7011, Jun. 2021, <https://doi.org/10.1109/TPEL.2020.3034246>.
- [2] R.-J. Wai and K.-M. Lin, "Robust decoupled control of direct field-oriented induction motor drive," *IEEE Transactions on Industrial Electronics*, vol. 52, no. 3, pp. 837–854, Jun. 2005, <https://doi.org/10.1109/TIE.2005.847585>.
- [3] D. Zellouma, Y. Bekakra, and H. Benbouhenni, "Field-oriented control based on parallel proportional–integral controllers of induction motor drive," *Energy Reports*, vol. 9, pp. 4846–4860, Dec. 2023, <https://doi.org/10.1016/j.egy.2023.04.008>.
- [4] M. A. Hannan, J. A. Ali, A. Mohamed, and A. Hussain, "Optimization techniques to enhance the performance of induction motor drives: A review," *Renewable and Sustainable Energy Reviews*, vol. 81, pp. 1611–1626, Jan. 2018, <https://doi.org/10.1016/j.rser.2017.05.240>.
- [5] G. Abid, S. A. Shaikh, M. F. Shaikh, S. Hafeez Rajput, U. A. Majeed, and A. M. Shaikh, "IoT based Smart Industrial panel for controlling Three-phase Induction motor," in *2020 3rd International Conference on Computing, Mathematics and Engineering Technologies*, Sukkur, Pakistan, 2020, pp. 1–8, <https://doi.org/10.1109/iCoMET48670.2020.9073809>.
- [6] U. Syarah and M. Yuhendri, "Constant Torque Control of Induction Motor Using Variable Frequency Drive Based on Internet of Things," *Journal of Industrial Automation and Electrical Engineering*, vol. 1, no. 1, pp. 7–12, Jul. 2024.
- [7] R. Azizipah-Anbarghoee and M. Malekpour, "Smart Induction Motor Variable Frequency Drives for Primary Frequency Regulation," *IEEE Transactions on Energy Conversion*, vol. 35, no. 1, pp. 1–10, Mar. 2020, <https://doi.org/10.1109/TEC.2019.2952318>.
- [8] R. Mudundi and M. K. Kumar, "Variable Frequency Drive Optimization with Adaptive Neuro Fuzzy Inference System," *International Journal of Integrated Engineering*, vol. 16, no. 3, pp. 333–345, Nov. 2024, <https://doi.org/10.30880/2021.10.12.04>.
- [9] A. Hareesh and B. Jayanand, "Scalar and Vector Controlled Infinite Level Inverter (ILI) Topology Fed Open-Ended Three-Phase Induction Motor," *IEEE Access*, vol. 9, pp. 98433–98459, 2021, <https://doi.org/10.1109/ACCESS.2021.3096125>.
- [10] Y. S. Kumar and G. Poddar, "Medium-Voltage Vector Control Induction Motor Drive at Zero Frequency Using Modular Multilevel Converter," *IEEE Transactions on Industrial Electronics*, vol. 65, no. 1, pp. 125–132, Jan. 2018, <https://doi.org/10.1109/TIE.2017.2721927>.
- [11] A. Datta and G. Poddar, "Improved Low-Frequency Operation of Hybrid Inverter for Medium-Voltage Induction Motor Drive Under V/f and Vector Control Mode of Operation," *IEEE Journal of Emerging and Selected Topics in Power Electronics*, vol. 8, no. 2, pp. 1248–1257, Jun. 2020, <https://doi.org/10.1109/JESTPE.2019.2903746>.
- [12] S. M. Goda, Y. S. Elkoteshy, A. N. Ouda, and A. E. Elawa, "Scalar Control Technique for Three Phase Induction Motor for Electric Vehicle Application," in *2018 Twentieth International Middle East Power Systems Conference*, Cairo, Egypt, 2018, pp. 705–711, <https://doi.org/10.1109/MEPCON.2018.8635187>.
- [13] F. Wang, Z. Zhang, X. Mei, J. Rodríguez, and R. Kennel, "Advanced Control Strategies of Induction Machine: Field Oriented Control, Direct Torque Control and Model Predictive Control," *Energies*, vol. 11, no. 1, Jan. 2018, Art. no. 120, <https://doi.org/10.3390/en11010120>.
- [14] G. Kamalapur and M. S. Aspalli, "Direct torque control and dynamic performance of induction motor using fractional order fuzzy logic controller," *International Journal of Electrical and Computer Engineering (IJECE)*, vol. 13, no. 4, pp. 3805–3816, Aug. 2023, <https://doi.org/10.11591/ijece.v13i4.pp3805-3816>.

- [15] A. P. Biswal and S. Satpathy, "Vector Control of 3-Phase Induction Motor," in *2021 1st Odisha International Conference on Electrical Power Engineering, Communication and Computing Technology*, Bhubaneswar, India, 2021, pp. 1–4, <https://doi.org/10.1109/ODICON50556.2021.9428930>.
- [16] R. Nair and G. Narayanan, "Emulation of Wind Turbine System Using Vector Controlled Induction Motor Drive," *IEEE Transactions on Industry Applications*, vol. 56, no. 4, pp. 4124–4133, Jul. 2020, <https://doi.org/10.1109/TIA.2020.2987993>.
- [17] J. Druant, F. De Belie, P. Sergeant, and J. Melkebeek, "Field-Oriented Control for an Induction-Machine-Based Electrical Variable Transmission," *IEEE Transactions on Vehicular Technology*, vol. 65, no. 6, pp. 4230–4240, Jun. 2016, <https://doi.org/10.1109/TVT.2015.2496625>.
- [18] S. Khadar, H. Abu-Rub, and A. Kouzou, "Sensorless Field-Oriented Control for Open-End Winding Five-Phase Induction Motor With Parameters Estimation," *IEEE Open Journal of the Industrial Electronics Society*, vol. 2, pp. 266–279, 2021, <https://doi.org/10.1109/OJIES.2021.3072232>.
- [19] R. Bojoi, P. Guglielmi, and G.-M. Pellegrino, "Sensorless Direct Field-Oriented Control of Three-Phase Induction Motor Drives for Low-Cost Applications," *IEEE Transactions on Industry Applications*, vol. 44, no. 2, pp. 475–481, Mar. 2008, <https://doi.org/10.1109/TIA.2008.916735>.
- [20] K. Szabat, T. Orlowska-Kowalska, and M. Dybkowski, "Indirect Adaptive Control of Induction Motor Drive System With an Elastic Coupling," *IEEE Transactions on Industrial Electronics*, vol. 56, no. 10, pp. 4038–4042, Oct. 2009, <https://doi.org/10.1109/TIE.2009.2022514>.
- [21] S. Potturi and R. P. Mandi, "Critical Survey on IOT Based Monitoring and Control of Induction Motor," in *2018 IEEE Student Conference on Research and Development*, Selangor, Malaysia, 2018, pp. 1–6, <https://doi.org/10.1109/SCORED.2018.8711222>.
- [22] M. Irfan, N. Saad, R. Ibrahim, and V. S. Asirvadam, "Development of an intelligent condition monitoring system for AC induction motors using PLC," in *2013 IEEE Business Engineering and Industrial Applications Colloquium*, Langkawi, Malaysia, 2013, pp. 789–794, <https://doi.org/10.1109/BEIAC.2013.6560243>.
- [23] G. Pavithra and Vinayak. V. Rao, "Remote Monitoring and Control of VFD fed Three Phase Induction Motor with PLC and LabVIEW software," in *2018 2nd International Conference on I-SMAC (IoT in Social, Mobile, Analytics and Cloud)*, Palladam, India, 2018, pp. 329–335, <https://doi.org/10.1109/I-SMAC.2018.8653657>.
- [24] D. Kalel and R. Raja Singh, "IoT integrated adaptive fault tolerant control for induction motor based critical load applications," *Engineering Science and Technology, an International Journal*, vol. 51, Mar. 2024, Art. no. 101585, <https://doi.org/10.1016/j.jestch.2023.101585>.
- [25] M. G. Ioannides *et al.*, "Design and Operation of Internet of Things-Based Monitoring Control System for Induction Machines," *Energies*, vol. 16, no. 7, Apr. 2023, Art. no. 3049, <https://doi.org/10.3390/en16073049>.
- [26] V. Seenivasan, K. Ponkumar, R. Venkatraman, and J. Jeslindrusilanesamalar, "Induction Motor Condition Monitoring and Controlling Based on IoT," *International Research Journal of Engineering and Technology*, vol. 6, no. 2, pp. 7157–7162, Mar. 2019.
- [27] M. G. Ioannides, A. P. Stamelos, Stylianos A. Papazis, E. E. Stamataki, and M. E. Stamatakis, "Internet of Things-Based Control of Induction Machines: Specifics of Electric Drives and Wind Energy Conversion Systems," *Energies*, vol. 17, no. 3, Feb. 2024, Art. no. 645, <https://doi.org/10.3390/en17030645>.
- [28] D. Shyamala, D. Swathi, J. L. Prasanna, and A. Ajitha, "IoT platform for condition monitoring of industrial motors," in *2017 2nd International Conference on Communication and Electronics Systems*, Coimbatore, India, 2017, pp. 260–265, <https://doi.org/10.1109/CESYS.2017.8321278>.
- [29] M. Jaishree, P. Navina, V. Naumitha Prebha, and P. Priyadarshini, "IoT Assisted Motor Monitoring System for Industries," in *2021 7th International Conference on Advanced Computing and Communication Systems*, Coimbatore, India, 2021, pp. 689–691, <https://doi.org/10.1109/ICACCS51430.2021.9441950>.
- [30] E. Noyjeen, C. Tanita, N. Panthasarn, P. Chansri, and J. Pukkham, "Monitoring Parameters of Three-Phase Induction Motor Using IoT," in *2021 9th International Electrical Engineering Congress*, Pattaya, Thailand, 2021, pp. 483–486, <https://doi.org/10.1109/IEECON51072.2021.9440368>.
- [31] X. Zhao, H. Liu, J. Zhang, and H. Zhang, "Simulation of Field Oriented Control in Induction Motor Drive System," *Indonesian Journal of Electrical Engineering and Computer Science*, vol. 11, no. 12, pp. 7555–7563, Dec. 2013.
- [32] B. Saad and A. Goléa, "Direct Field-Oriented Control using Fuzzy Logic Type -2 for Induction Motor with Broken Rotor Bars | IIETA," vol. 72, no. 1, pp. 1–10, Feb. 2017, https://doi.org/10.18280/ama_c.720101.
- [33] A. Bounab, A. Chaiba, and S. Belkacem, "Evaluation of the High Performance Indirect Field Oriented Controlled Dual Induction Motor Drive Fed by a Single Inverter using Type-2 Fuzzy Logic Control," *Engineering, Technology & Applied Science Research*, vol. 10, no. 5, pp. 6301–6308, Oct. 2020, <https://doi.org/10.48084/etasr.3799>.